NeuroImage: Clinical 29 (2021) 102530

Contents lists available at ScienceDirect

NeuroImage: Clinical

journal homepage: www.elsevier.com/locate/ynicl

Multi-modal biomarkers of low back pain: A machine learning approach

Bidhan Lamichhane [a,1], Dinal Jayasekera [b,1,*], Rachel Jakes [b], Matthew F. Glasser [c,d], Justin Zhang [a], Chunhui Yang [d], Derayvia Grimes [a], Tyler L. Frank [a], Wilson Z. Ray [a,b], Eric C. Leuthardt [a,b,d], Ammar H. Hawasli [a,e]

[a] Department of Neurosurgery, Washington University School of Medicine, St. Louis, MO 63110, USA
[b] Department of Biomedical Engineering, Washington University in St. Louis McKelvey School of Engineering, St. Louis, MO 63130, USA
[c] Department of Radiology, Washington University School of Medicine, St. Louis, MO 63110, USA
[d] Department of Neuroscience, Washington University School of Medicine, St. Louis, MO 63110, USA
[e] Meritas Health Neurosurgery, North Kansas City 64116, USA

ARTICLE INFO

Keywords:
Low back pain
Cortical thickness
Resting state connectivity
Support vector machine
Pain processing
Emotion processing

ABSTRACT

Chronic low back pain (LBP) is a very common health problem worldwide and a major cause of disability. Yet, the lack of quantifiable metrics on which to base clinical decisions leads to imprecise treatments, unnecessary surgery and reduced patient outcomes. Although, the focus of LBP has largely focused on the spine, the literature demonstrates a robust reorganization of the human brain in the setting of LBP. Brain neuroimaging holds promise for the discovery of biomarkers that will improve the treatment of chronic LBP. In this study, we report on morphological changes in cerebral cortical thickness (CT) and resting-state functional connectivity (rsFC) measures as potential brain biomarkers for LBP. Structural MRI scans, resting state functional MRI scans and self-reported clinical scores were collected from 24 LBP patients and 27 age-matched healthy controls (HC). The results suggest widespread differences in CT in LBP patients relative to HC. These differences in CT are correlated with self-reported clinical summary scores, the Physical Component Summary and Mental Component Summary scores. The primary visual, secondary visual and default mode networks showed significant age-corrected increases in connectivity with multiple networks in LBP patients. Cortical regions classified as hubs based on their eigenvector centrality (EC) showed differences in their topology within motor and visual processing regions. Finally, a support vector machine trained using CT to classify LBP subjects from HC achieved an average classification accuracy of 74.51%, AUC = 0.787 (95% CI: 0.66–0.91). The findings from this study suggest widespread changes in CT and rsFC in patients with LBP while a machine learning algorithm trained using CT can predict patient group. Taken together, these findings suggest that CT and rsFC may act as potential biomarkers for LBP to guide therapy.

1. Introduction

Chronic low back pain (LBP) represents a significant public health problem and is a major cause of disability globally (Vos et al., 2017). Health care costs for LBP in the United States have ballooned to nearly $1 trillion dollars (Dieleman et al., 2016). The diagnosis and treatment of chronic LBP has been complicated by heterogenous etiologies and neuroimaging modalities that fail to measure central mechanisms of pain (Rudisch et al., 1998; Thomsen et al., 2001; Vaccaro et al., 1994). Spinal magnetic resonance imaging (MRI) techniques are actively utilized in the investigation of biomarkers of LBP but are often limited by artifacts imposed by spinal implants necessary for stabilization and also do not measure central pain processing mechanisms (Rudisch et al., 1998; Thomsen et al., 2001). In fact, it is well known that many individuals with LBP show no significant abnormalities in modern spinal imaging (Rubinstein and van Tulder, 2008). These hurdles and the complex pathophysiology of chronic LBP make its prognostication and clinical management challenging (Last and Hulbert, 2009).

Brain imaging has identified regions that are involved in the processing and perception of pain (Martucci and Mackey, 2018; Yarkoni et al., 2011). The cortical areas identified are involved in motor processing (primary motor cortex, supplementary motor area),

* Corresponding author.
E-mail address: dinal.jayasekera@wustl.edu (D. Jayasekera).
[1] These authors contributed equally to this work.

https://doi.org/10.1016/j.nicl.2020.102530
Received 31 August 2020; Received in revised form 3 December 2020; Accepted 5 December 2020
Available online 8 December 2020

multisensory integration (temporal-parietal junction), cognitive perception of pain (anterior cingulate cortex, ventromedial prefrontal cortex, dorsolateral prefrontal cortex), and act as nociceptive centers of pain (insula, thalamus). However, neural correlates of LBP remain poorly understood. Cortical thickness (CT) appears to reflect the functional organization of the human cortex and act as a potential marker for the development of LBP. Regional changes in grey matter have been reported in several pain studies (Bagarinao et al., 2014; Bernabéu-Sanz et al., 2020). Baliki et al. demonstrated a global reduction in grey matter volume and a disruption of the whole-brain morphological organization in LBP patients (Baliki et al., 2011). They also showed that subjects who clinically recovered had normal gray matter volumes, but subjects with persistent LBP demonstrated global and regional reductions in gray matter volume (Baliki et al., 2012).

In addition to biomarkers derived from structural MRI, resting state functional MRI (rsfMRI) has gained immense popularity in measuring functional connectivity between brain regions and resting state networks (RSN) in patients with LBP (Shen et al., 2019). Experiments have reported disruptions in connectivity within the visual processing stream (Shen et al., 2019) and between the insula and pain processing areas (Wiech et al., 2014) of LBP patients. Similar observations have been reported on connectivity between the nucleus accumbens and medial prefrontal cortex (Baliki et al., 2012; Hashmi et al., 2013). Furthermore, there is increasing evidence from other neurological disorders that damage to one part of the central nervous system (CNS) can disrupt connectivity patterns within other CNS structures (Carrera and Tononi, 2014). This can lead to disturbances in network connectivity on a global brain level. However, previous studies lack a systematic analysis of global patterns of rsFC, and the brain's intra- and inter-network interactions in LBP.

Patterns of resting state connectivity can also be modeled using graph theoretical measures consisting of nodes (brain parcels) and edges (functional interactions between brain regions). The organization of these RSNs is critical to the flow of information between nodes and its resulting efficiency. Hubs play a key role in facilitating more efficient integration of information between nodes by adopting a highly connected and functionally central role within a network (van den Heuvel and Sporns, 2013). Changes have been reported in the network organization of individuals with chronic pain disorders (Balenzuela et al., 2010; De Pauw et al., 2020; Liu et al., 2012) and LBP (Mansour et al., 2016) However, these studies did not examine hubs specifically. Instead, they assessed the variability in node community membership. The highly-connected nature of hubs creates an inherent vulnerability in the event of a disruption to its organization. This can result in significant interruption in the flow of information. In fact, hubs are disproportionally affected in neurological disorders as changes in CT are more likely to occur in hubs (Crossley et al., 2014; Stam, 2014).

When taken together, the literature demonstrates that LBP patients show differences on a structural and functional level within the brain. We hypothesized that patients with LBP will show disruptions in functional connectivity between brain regions involved in the processing and perception of pain. We further hypothesized that LBP patients would show aberrations in the CT within regions previously implicated in the processing of pain and that these changes would predict subject-reported clinical pain scores. Additionally, we set out to examine if variations in CT could be used as an imaging biomarker to train machine learning algorithms to classify LBP from healthy controls. Thus, the aims of this study were to 1) characterize the cortical areas that showed age-corrected differences in cortical thickness between patient groups, 2) determine associations between CT with self-reported clinical summary scores, 3) characterize differences in functional connectivity on a cortical area and network level, 4) examine global network properties and hub topology, and 5) train a support vector machine to accurately predict LBP from healthy controls and support a clinical translation of this technique.

We collected high-resolution structural and resting state scans and self-reported clinical data for the 36-Item Short Form healthy survey (SF-36). We used the Human Connectome Project's (HCP) multi-modal surface-based cortical parcellation (MMP) which contains 180 symmetric cortical parcels per hemisphere (Glasser et al., 2016a). This parcellation is defined in terms of surface vertices and used across multiple modalities to define cortical areal borders, making it possible to accurately map the parcellation to individual subjects.

2. Methods

2.1. Participants

Participants were recruited through the Washington University School of Medicine Research Participant Registry (Volunteer for Health) and direct patient contact during hospital visits at the Barnes Jewish Hospital, Washington University School of Medicine, and Barnes Jewish West County Hospital. Prior to enrollment in the study, a trained physician screened prospective participants. LBP patients with a history of LBP over 6 months without lower extremity symptoms were recruited for this study. LBP subjects had a diagnosis of chronic low back pain due to lumbar spondyloarthropathy without history of lumbar spine surgery. All eligible healthy controls (HC) in the study had no history of neurological injury or disease at the time of scanning.

All procedures used in this study were approved by the Washington University in St. Louis Institutional Review Board. Written informed consent was obtained from all participants prior to MRI scanning and administration of clinical surveys. A sample of 27 HC and 24 LBP subjects (age matched; $p = 0.21$, Wilcoxon rank-sum test) were recruited for the study (refer ***Supplementary Information*** ***Methods*** for inclusion and exclusion criteria).

2.2. Clinical surveys and factor analysis

Data for the Short-Form 36-item (SF-36) health survey questionnaire (Ware and Sherbourne, 1992) was collected from each participant. The SF-36 is summarized into 8 sub-categories 1) physical functioning (PF), 2) role limitations due to physical health problems (RLP), 3) bodily pain (P), 4) general health (GH), 5) energy fatigue (EF), 6) social functioning (SF), 7) role limitations due to emotional problems (RLE) and 8) emotional well-being (E) (Ware, 1993). A higher score for any of these categories represents a better health condition for these 8 subcategories.

These eight scales can be aggregated into physical and mental component summary scores (Ware et al., 1994). Scores for the eight SF-36 subscales were calculated following the standard guideline (Ware, 1993; Ware and Sherbourne, 1992). A factor analysis approach was then applied to these scores to get the Physical Component Summary (PCS) factor score, and the Mental Component Summary score (MCS) as used in previous studies (Farivar et al., 2007; Ware et al., 1994, 1995).

2.3. MRI and fMRI data acquisition and pre-processing

All MRI data were collected in a 3T Siemens Prisma and 32-channel head coil; 0.8 mm isotropic T1-weighted and T2-weighted scans were obtained. The functional runs were collected using multi-band gradient echo EPI (Multi band accel. factor = 6). The entire brain was scanned with high spatial (2.4 × 2.4 mm × 2.4 mm) and temporal (TR = 800 ms) resolution (repetition time [TR] = 800 ms, echo time [TE] = 33 ms and flip angle = 52°). A 2.4 mm isotropic spin echo field map that is matched to the fMRI acquisition was obtained to correct the fMRI data for distortion. Six resting state fMRI scans, each approximately 5 min long, with AP/PA phase encoding directions (60 axial slices each) were collected. T1- and T2-weighted sequences were collected using volumetric navigator sequences which prospectively corrected for motion by repeating scans (Tisdall et al., 2012). While collecting the resting scans, subjects were asked to focus their attention on a visual cross-hair and remain awake.

Preprocessing of multi-modal MRI data was done using the Human Connectome Project's minimal preprocessing pipeline (v4.0.0) (Glasser

et al., 2018, 2016a, 2016b, 2013; Robinson et al., 2018) including the PreFreeSurfer, FreeSurfer, and PostFreeSurfer HCP Structural Preprocessing Pipelines for generating subcortical segmentation and cortical surfaces; functional preprocessing and denoising pipelines, which include the fMRIVolume, fMRISurface, and multi-run spatial ICA + FIX pipelines that correct for motion and distortions within fMRI data by mapping it into a standard CIFTI grayordinate space and removing spatially specific structured noise; and the MSMAll areal-feature-based cross-subject surface registration pipeline for precisely aligning the individual subjects' cortical areas to the HCP's multi-modal parcellation. Temporal ICA (Glasser et al., 2019, 2018) was used to clean the MSMAll aligned resting state fMRI data of global noise after spatial ICA had been used to clean the data of spatially specific noise (see ***Supplementary Information Methods***).

2.4. Acquisition and analysis of cortical thickness (CT) data

To sample data at the areal level, we used the HCP's MMP (Glasser et al., 2016a). This parcellation contains 180 symmetric cortical areas per hemisphere totaling 360 parcels. For each subject, the average cortical gray matter thickness value was extracted (Fischl and Dale, 2000; Greve and Fischl, 2018) from each of the 360 parcels that had been functionally aligned to the individual data with MSMAll. Multiple regression was used to determine if each cortical area's thickness differed significantly ($p < 0.05$) between patients with LBP and healthy controls while controlling for age.

2.5. Resting state functional connectivity (rsFC) analysis

A functional connectome for each subject was generated by taking the average timeseries in each of 360 cortical areas and taking the Fisher-z transformed Pearson's correlation between each pair of cortical areas. The functional connectome was reordered so that cortical areas were grouped within one of 12 RSNs from Ji et al.(Ji et al., 2019). These RSNs were the primary visual (VIS1), secondary visual (VIS2), auditory (AUD), somatomotor (SOM), cingulo-opercular (CON), default-mode (DMN), dorsal attention (DAN), frontoparietal cognitive control (FPN), posterior multimodal (PML), ventral multimodal (VML), language (LAN), and orbito-affective (OA) networks.

Differences in parcel-to-parcel connectivity were tested using a Wilcoxon rank-sum test and the corresponding z values determined. To assess differences in connectivity between networks, the parcels of the Fisher-z transformed Pearson's correlation matrix were reorganized based on its membership in a specific network and the corresponding average connectivity was computed for each network. The differences in network connectivity were then tested using a Wilcoxon rank-sum test.

2.6. Graph theoretical analyses

Each parcel of the HCP's MMP was modelled as a node, resulting in a total of 360 non-overlapping nodes. Thresholding a connectivity matrix based on correlation strength can yield different network densities which can in turn influence network properties that bias graph metric comparisons between patient populations (Bassett et al., 2012; Ginestet et al., 2011; Schwarz and McGonigle, 2011). Therefore, we decided to threshold all graphs at the same network densities by taking a percentage of all the positive connections and binarizing the graphs prior to calculating any graph theory metrics. Binarization is used in functional graphs (Achard and Bullmore, 2007; Supekar et al., 2008) to preserve only the most probable functional connections and treat these connections equivalently. As there is no accepted cutoff for functional connectivity strength to determine whether a functional connection is nontrivial, we thresholded connections in Fisher-z transformed matrices within the top 15% for each individual, in steps of 2.5% up to 30% density, to create binary undirected graphs for each network density.

Using the Brain Connectivity Toolbox (Rubinov and Sporns, 2010), we calculated the global graph metrics: global efficiency, clustering coefficient, and characteristic path length for each patient which provide an estimate of how easily information can be integrated across the network. The *characteristic path length* (the average smallest number of edges between all pairs of nodes in the graph that never visit a single node more than once) measures how easily information can be transferred across the network. The *global efficiency* (the average inverse shortest path length in the network) is a test of the ability of parallel information processing over brain networks. The *clustering coefficient* (the fraction of triangles around a network) is a measure of how well connected the neighbors of a node are to each other. We averaged these metrics across thresholds for each node as previously published (Achard et al., 2012; Kaplan et al., 2019; Lynall et al., 2010).

We determined the network efficiency, at the global level, of each RSN for each patient by calculating its global efficiency. This provides an estimate of parallel information transformation and global functioning within a specific RSN. We extracted the thresholded and binarized connectome for each intra-network interaction at each network density and calculated the global efficiency of each RSN rsFC matrix for each patient using the Brain Connectivity Toolbox (Rubinov and Sporns, 2010). Differences in the global efficiency of each RSN were tested using a Wilcoxon rank-sum test and the corresponding z values determined.

2.7. Identification of hubs

Hubs can be identified using different graph theory measures such as degree (number of connections a node has) or centrality (relative importance of a node with respect to its surrounding nodes in propagating the information to other nodes in the network). Eigenvector centrality is a centrality measure of how well connected one node is to other nodes that are well connected (Fornito et al., 2016). We chose eigenvector centrality to classify hubs due to its more self-referential nature. We calculated the eigenvector centrality for each parcel in each patient using the Brain Connectivity Toolbox (Rubinov and Sporns, 2010). These values were then averaged across patients for each parcel to form a group average for LBP patients and HC. Hub status was assigned to nodes whose eigenvector centrality was one standard deviation above the group mean (Kaplan et al., 2019). We identified parcels that were found to be hubs in 1) both LBP patients and HC, 2) only HC and not in LBP patients, and 3) only LBP patients and not in HC.

2.8. Machine assisted classification

A support vector machine (SVM) classifier, with a linear kernel, was used due to its established predictive power with relatively small sample sizes (Arslan et al., 2016). We used the caret package available within RStudio (rstudio.com) to implement our machine learning classifier (Kuhn, 2008). We used leave-one-out (LOO) cross-validation to test the performance of our SVM due to the limited number of patients in the present study. The steps involved in the SVM classification analysis are briefly discussed below. It is important to note that the feature selection, parameter optimization and final model training, in each LOO iteration, was performed on the training dataset which included all subject data except for one (the left-out subject or the test subject).

2.8.1. Feature reduction

We used 360 features (one cortical thickness value for each of the 360 parcels) with a relatively small sample size (subject number = 51). We used a dimensionality reduction approach as the dimensions (number of features) of the data were much larger than the sample size. This method is called feature selection (or reduction) and is essential to high-dimensional data, a common problem in neuroimaging (Saeys et al., 2007), to avoid over fitting. We aimed to keep relevant features and remove relatively insignificant feature variables to achieve a higher classification performance when testing data and a better generalization

to independent datasets. We used recursive feature elimination (RFE) (Guyon et al., 2002) in this study. RFE is a popular feature selection approach that is effective in data dimension reduction, increases efficiency of MRI datasets (Arbabshirani et al., 2017; Blum and Langley, 1997; Hall and Smith, 1998; Kohavi and John, 1997), and is applied in many neuroimaging studies (Qiao et al. 2019). RFE aids in the elimination of redundant features without incurring substantial loss of information and enables set important features to be used in SVM model training. Within the RFE framework, we used 4-fold cross-validation with ten repetitions to get most of the data patterns from the training set and to obtain a best predicting feature subset.

2.8.2. Model training and classification of test subject(s)

In the model-training phase, RFE-selected features were used to train the SVM model. As with many other supervised machine learning approaches, the SVM algorithm performs poorly on experimental data when the default parameter values are used. Accordingly, the training set was utilized to determine the optimal parameters of the SVM classifier and to build the best performing SVM model. The model parameter (the cost in the case of linear SVM) is optimized to maximally discriminate one group from another (HC from LBP group) by using the grid-search algorithm. In the present study, the search scale was c = 1:10. After the grid-search, the best performing cost was used in the final model. The performance of the SVM model was trialed using a testing data set (left-out subject's data) in each LOO iteration.

2.8.3. Evaluation of overall performance (accuracy, sensitivity, specificity and AUC)

The output of a binary classifier is viewed as a confusion matrix (***Supplementary Information, Table S1***). The accuracy percentage (%) is defined as the ratio of the number of accurately classified subjects to the total number of subjects {(TP + TN)/(TP + TN + FP + FN)}. In addition to accuracy, the specificity and the sensitivity values are also reported. Sensitivity (the proportion of correctly classified positive samples out of all positive returns, or the true positive rate) indicates the accuracy of the prediction group {TP/(TP + FN)}, which in this case is the HC group. Specificity (the proportion of correctly classified negative samples out of all negative returns, or true negative rate), calculated as {TN/(TN + FP)}, indicates the accuracy of the prediction of the absence group, which in this case is the LBP group. To evaluate overall model performance, we performed an area under the ROC (Receiver Operating Characteristics curve) analysis, more commonly referred to as an area under the curve (AUC) analysis.

2.9. Statistical tests

An unpaired two-sample Wilcoxon rank-sum test with $p < 0.05$ was used to evaluate statistically significant differences for group comparisons in both structural and functional data. To correct for multiple comparisons, we used False Discovery Rate Correction (FDR) with $q < 0.05$.

3. Results

3.1. Clinical surveys

We compared the LBP SF-36 summary scale scores to HC using a non-parametric Wilcoxon rank-sum test. There were statistically significant ($p < 0.05$) differences in sub-scores between patient groups except for the RLE sub-score (Table 1). Higher differences were seen in the physical domains (PF, RLP, P, and GH) than in the emotional domain (EF, SF, RLE, EW). This shows that LBP leads to greater impairment of physical than mental functioning.

To reduce the dimensionality of the SF-36 data, we then calculated factor summary scores (PCS and MCS) for the eight SF-36 subscales (see methods *Section 2.2* for more details). The oblique two-factor solution indicated that physical functioning (PF), role limitations due to physical health problems (RLP), bodily pain (P), general health (GH), and social functioning (SF) loaded heavily on the Physical Component Summary (PCS) factor score whereas energy and fatigue (EF), role limitation due to emotional problem (RLE) and emotional well-being (EW) loaded most heavily on the Mental Component Summary (MCS) scores (***Supplementary Information*** Table 2).

Table 1
Participant demographic and clinical information. A Wilcoxon rank-sum test was used to find differences in SF-36-subscores between HC and LBP. Higher scores indicate healthier functioning. PF = physical functioning, RLP = role limitations due to physical health problems, P = bodily pain, GH = general health, EF = energy and fatigue, SF = social functioning, RLE = role limitations due to emotional problems, EW = emotional well-being. (* = $p < 0.05$, ** = $p < 0.01$, *** = $p < 0.001$; p values have been corrected for multiple comparisons using FDR).

Variable	Healthy Controls	LBP
Participants (n)	27	24
Sex (M/F)	15/12	9/15
Age (in years)	46.9 ± 17.3	53.5 ± 10.2
SF-36 PF score***	53.47 ± 28.5	92.3 ± 17.7
SF-36 RLP score***	46.87 ± 43.5	94.4 ± 14.4
SF-36P score***	48.96 ± 17.22	86.57 ± 16.7
SF-36 GH score***	58.86 ± 19.22	80.56 ± 15.1
SF-36 EF score*	53.95 ± 19.4	66.30 ± 18.2
SF-36 SF score**	70.83 ± 24.90	91.67 ± 14.7
SF-36 RLE score	83.32 ± 32.6	95.05 ± 17.8
SF-36 EW score*	72.67 ± 17.1	82.81 ± 11.4

We computed the summary scores for the PCS and MCS scores for each subject to use in further analysis as pain and emotion scores. Multivariate analyses were used to assess the relationship between CT, and PCS and MCS scores separately after correcting for age (see *Section 3.3* for details).

3.2. Changes in cortical thickness

There were widespread differences, both thinning and thickening, in CT between the two groups. The age-corrected beta parameters for the group differences (the group- as predictor) from the multiple regression analysis (see *Section 2.4*) were plotted in Fig. 1. The parcels colored in red are thinner in LBP (LBP < HC). The parcels that are thicker in LBP (LBP > HC) are colored blue. The parcels with a significant group difference ($p < 0.05$, uncorrected) are outlined in black, and parcels that survived multiple comparison correction ($q < 0.05$) are outlined in green. In general, LBP subjects had widespread regions of thicker cortex within the bilateral occipital, temporal and parietal lobes. Notably, the posterior cingulate and temporal parietal junction in both hemispheres and the left motor and premotor sortices showed thicker cortex in LBP patients. (see ***Supplementary Information, Table S2*** for more details on significant parcels). These findings were also replicated by a vertex-wise analysis of CT (see ***Supplementary Information, Fig. S1***).

3.3. Association between cortical thickness and clinical summary scores

We tested the relationship of the PCS and MCS scores with CT using a linear regression model while controlling for age. Both clinical summary factors were independently found to be significant predictors (see ***Supplementary Information Tables 4 and 5*** for more details) of the CT of multiple cortical areas (Fig. 2, $p < 0.05$, age-controlled). There were widespread associations which were neither limited to specific functional networks nor specific cortical locations. We also tested the relationship of the PCS and MCS scores with CT within the LBP group (see ***Supplementary Information, Fig. S2A and S2B***).

A higher score for either the PCS or MCS suggests healthier functioning (see *Section 2.2*). A negative beta value from the regression (Fig. 2, blue regions) represents a region that shows a positive association

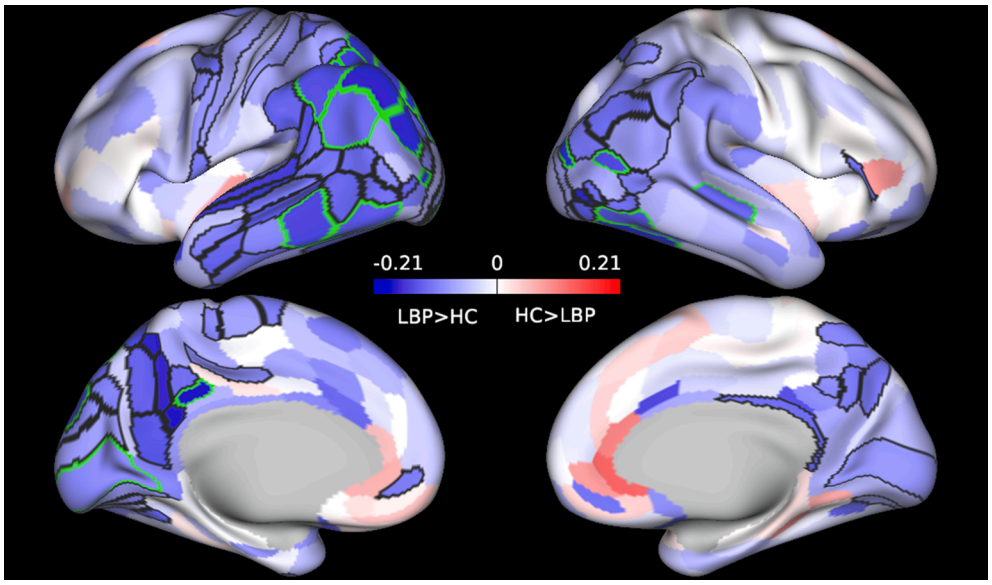

Fig. 1. Consequences of LBP on cortical thickness. The cortical map summarizes the weight (beta parameter) of group effect in CT. The positive beta (red) represents areas of thicker cortex in controls. The negative beta (blue) represent the cortex that is thicker in LBP compared to HC. The parcels outlined with a black boundary show significant group differences between HC and LBP ($p < 0.05$, uncorrected) and those outlined in green show significant group differences that survive FDR correction ($q < 0.05$). (For interpretation of the references to color in this figure legend, the reader is referred to the web version of this article.)

between the summary score and CT in LBP. Similarly, a positive beta value (red regions) represents a region that shows a negative association between the respective summary score and CT in LBP.

3.4. Parcel and network rsFC analysis

Differences in rsFC between LBP and HC were calculated as described in *Section 2.5*. Fig. 3**A** shows the parcels reordered by network that showed significant ($p < 0.05$ uncorrected) differences in connectivity. We also computed group differences of inter- and intra-network functional connectivity. There were multiple statistically significant differences in inter network connectivity interactions as shown in Fig. 3**B** (see ***Supplementary Information, Tables S6 and S7*** for more details). We determined that age was not a significant predictor of the network functional connectivity interactions (shown in Fig. 3**B)** using a linear regression analysis. Fig. 3**C** shows the resting state networks plotted on the cortical surface as outlined by the Cole-Anticevic Brain Network Parcellation (Ji et al., 2019).

3.5. LBP and HC had similar global graph metrics

There were no significant differences in global efficiency or clustering coefficient, of the reconstructed brain networks between LBP patients and HC (all $p > 0.05$, see ***Supplementary Information, Table S8***). However, there was a significant difference in the characteristic path length of the reconstructed brain networks between LBP patients and HC ($z = 2.236$, $p = 0.0253$). Global efficiency places a smaller influence on parcels that are isolated from the network when compared to characteristic path length (Latora and Marchiori, 2001; Rubinov and Sporns, 2010). Since we didn't observe a significant difference in the global efficiency between both patient cohorts, we can conclude that the reconstructed brain networks of LBP patients had more isolated parcels than HC.

3.6. Changes in network efficiency

We next investigated changes in network efficiency within each of the 12 resting state networks in LBP when compared with HC. There was a statistically significant decrease ($z = -2.10$, $p = 0.0320$ uncorrected) in the network efficiency of the default mode network (Fig. 4) in LBP and trending significant differences in the frontoparietal and ventral multimodal networks as shown in Table 2**.**

3.7. Nature of brain's hub structure in LBP

We calculated the eigenvector centrality of each node to investigate the nature of its connections with surrounding nodes. A hub was defined as a node whose eigenvector centrality was one standard deviation above the group mean. As a result, we identified hubs that were found in 1) both LBP and HC (see ***Supplementary Information, Table S9***), 2) HC but not in LBP (see ***Supplementary Information, Table S10***), and 3) LBP but not in HC (see ***Supplementary Information, Table S11***) and then matched each of the corresponding hubs to their respective resting state networks. The hubs for each of the three conditions were then projected onto a brain mesh surface (shown in Fig. 5).

3.8. Machine learning classification of LBP and HC groups

We used the cortical thickness (CT) as the feature to train a support vector machine to accurately classify each subject to their respective patient group (see methods *Section 2.8*). Table 3 summarizes the overall classification results. When classifying LBP from HC, we achieved a classification accuracy of 74.51%, AUC of 0.787 (95% CI: 0.66–0.91), sensitivity of 74.07%, and a specificity of 75.00%.

The receiver operating characteristic (ROC) curves for stratifying patients is shown in Fig. 6**A**. The cortical areas contributing to the classification and their corresponding frequency values, repetitions out of total (51 iterations in this study) LOO iterations, were plotted on a brain mesh surface (Fig. 6**B**, see ***Supplementary Information, Table S12*** for more details on individual parcels).

4. Discussion

In this study we identify structural and functional biomarkers in LBP patients by applying a multi-modal approach using a surface-based cortical parcellation. The results revealed the following in LBP patients: 1) Differences in CT between LBP and HC, 2) associations between CT and self-reported clinical scores, 3) decreased functional connectivity between multiple networks, 4) lower network efficiency of the default mode network, and 5) changes to hub topology of the brain. In addition, a support vector machine trained using CT values achieved a very high level of accuracy differentiating LBP from HC.

4.1. Cortical thickenss as a predictor of pain and emotion scores

Several studies have observed grey matter decreases with longer pain

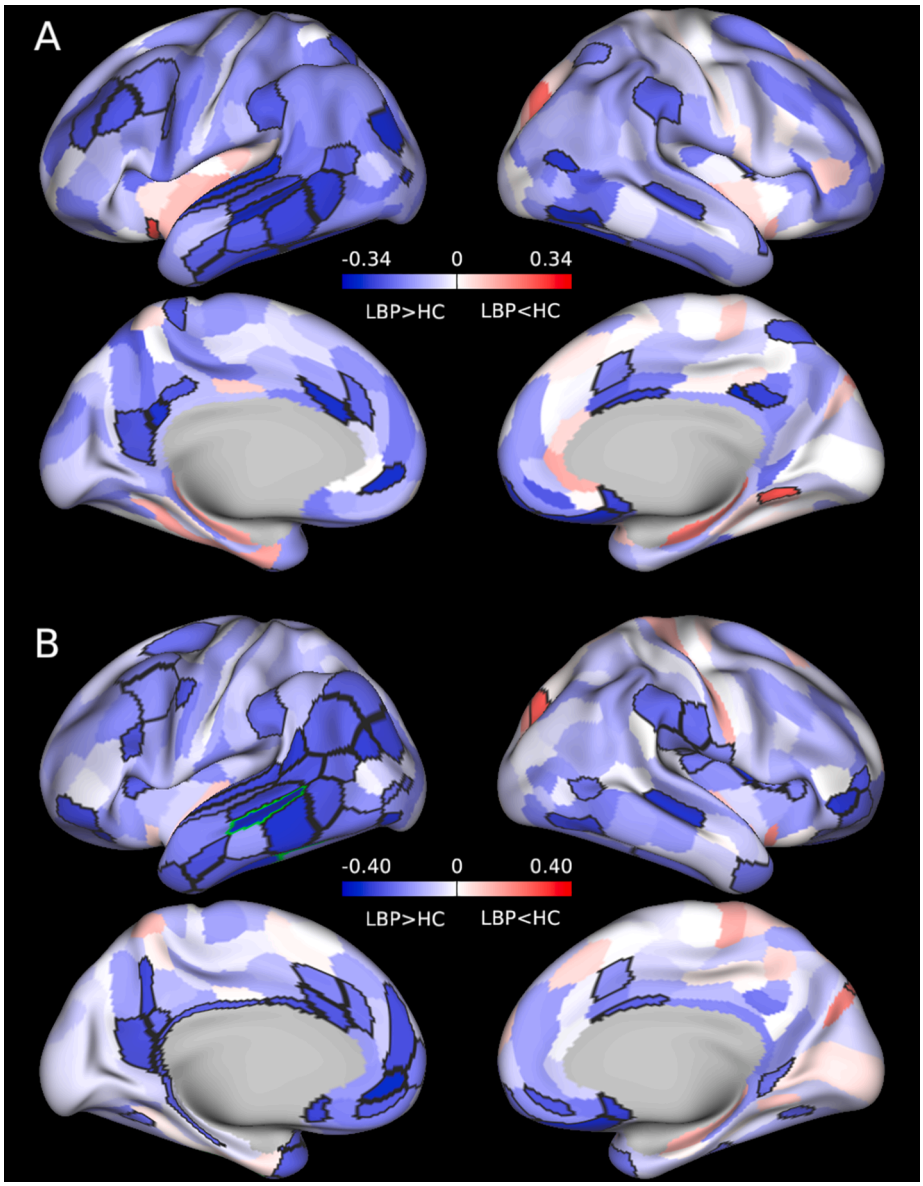

Fig. 2. Cortical thickness predicts subject-reported pain scores. The figure summarizes the beta parameter of the clinical factor score when predicting CT in a general linear model after correcting for age (age-adjusted regression analysis). A) Beta parameter of Physical Component Summary (PCS) factor scores, and B) Beta parameter of Mental Component Summary (MCS) factor scores. The parcels outlined in black are significantly correlated (predicted) with clinical factor scores ($p < 0.05$, uncorrected) and those outlined in green show significant group differences that survive FDR correction ($q < 0.05$). Since a higher clinical score suggests a better health condition, a negative beta (blue regions) suggests a thinner cortex in the HC group compared with LBP (thicker cortex in LBP). Similarly, the positive beta (red regions) suggests thicker cortical regions in HC (thinner cortex in LBP patients). (For interpretation of the references to color in this figure legend, the reader is referred to the web version of this article.)

duration in the dorsolateral prefrontal cortex, insular cortex, and anterior and dorsal anterior cingulate cortices (Apkarian et al., 2004; Kim et al., 2008; Lutz et al., 2008; Rocca et al., 2006; Schmidt-Wilcke et al., 2005; Valet et al., 2009). These areas have been described as vulnerable due to stress (Lutz et al., 2008; Schmidt-Wilcke et al., 2005; Valet et al., 2009), which may indicate that gray matter decreases are a consequence of chronic pain and anxiety that is not unique to LBP (Schmidt-Wilcke et al., 2005). In our study, decreases in the CT of these regions were not statistically significant in our LBP population. As reported in previous studies (Kong et al., 2013; Teutsch et al., 2008), there were significant increases in CT of the posterior parietal junction, temporal parietal junction, and visual-processing stream (FDR corrected $p < 0.05$, Fig. 1 and ***Supplementary Information, Table S3***) in our LBP cohort. In addition, the cortical areas contributing to the classification of patients using CT (Fig. 6**B** and ***Supplementary Information, Table S12***) were similar to findings by Ung et al. (Ung et al., 2014) in chronic LBP patients. These included regions such as the temporal, sensory-motor, cingulate and prefrontal cortices which are commonly implicated in pain processing.

We also tested the relationship between the degree of pain and emotion with CT (Burgmer et al., 2009; Ruscheweyh et al., 2011). The CT in the left dorsolateral prefrontal cortex, anterior cingulate cortex, midcingulate cortex, posterior cingulate cortex, posterior parietal cortex, and lateral temporal cortices predicted clinical pain scores (***Supplementary Information, Table S4***). LBP patients commonly exhibit emotional and cognitive disorders, including depression, anxiety, and sleep disturbances (Baliki et al., 2008). Appropriately, the parcels which predicted the subject-reported pain scores are known to be involved in the limbic processing of emotion and affective control in LBP patients (Baliki et al., 2008; Grachev et al., 2002; Letzen and Robinson, 2017).

There were many parcels showing significant correlations with both pain and emotion summary scores. The effects of pain and emotion are known to coexist in LBP and thus this overlap was expected to be seen in the neuronal circuitry of the brain. However, it is not known whether this overlap in pain and emotional scores reflects a common underlying pathophysiological process or mutually exclusive process. Few studies have documented increases in gray matter volume in the premotor cortex, midcingulate cortex, S1, inferior parietal lobule, and the medial temporal gyrus (Teutsch et al., 2008) in the presence of pain stimuli. Regions within the temporal lobe, including the medial and inferior temporal gyrus are associated with pain and emotion in studies using different paradigms, such as during emotion anticipation (Erk et al.,

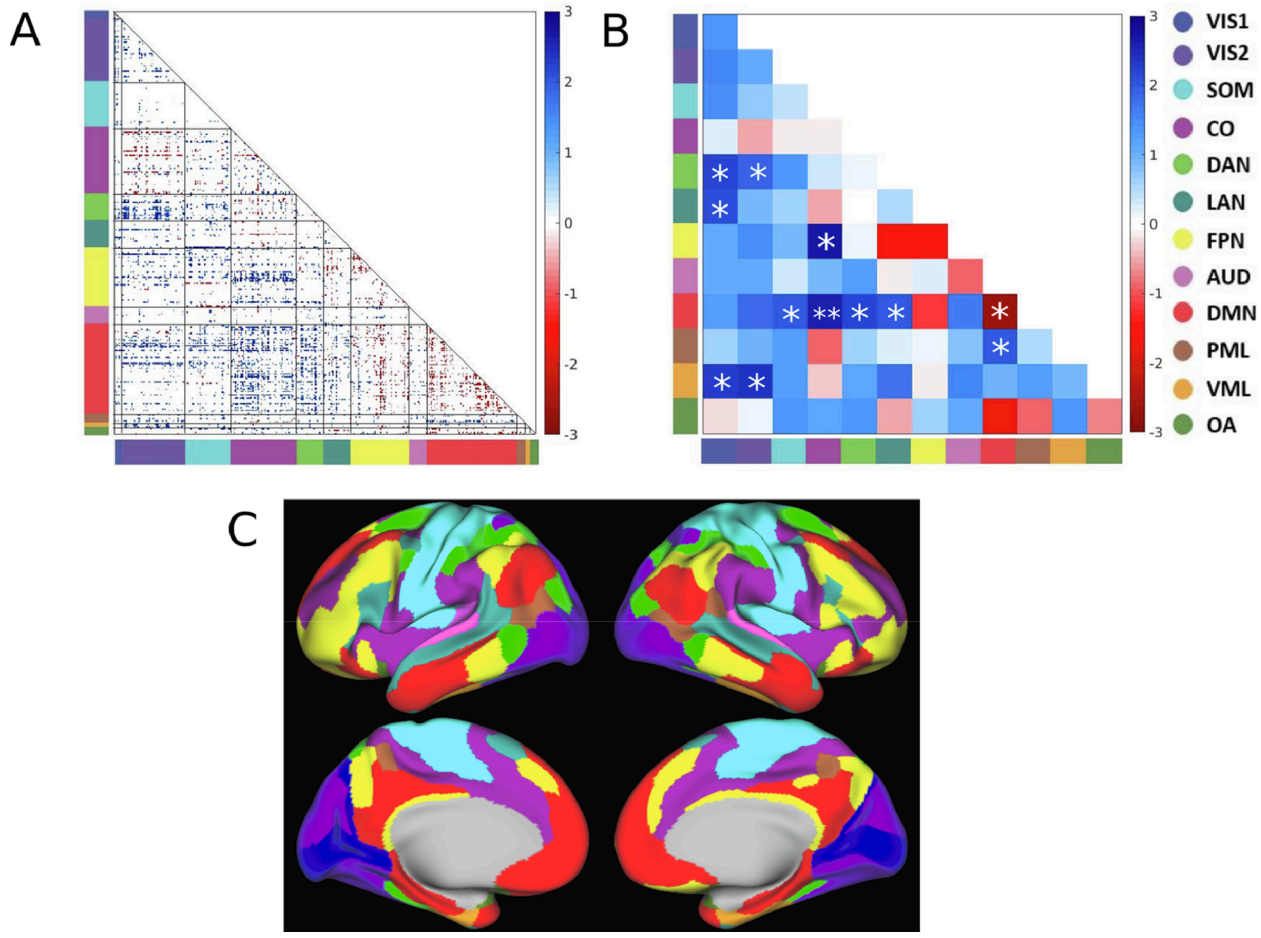

Fig. 3. Group differences in rsFC (Fisher's Z transformed) between LBP and HC groups. Note that red regions represent cortical areas or networks with reduced rsFC in LBP when compared to HC and blue regions represent increases. A) The lower triangle shows the z-scores for differences in rsFC between cortical areas grouped by network. A color code was assigned to significant ($p < 0.05$, uncorrected) differences. B) Difference in average connectivity between each pair of resting state networks in terms of z-values (* = $p < 0.05$, uncorrected; ** = $p < 0.001$, uncorrected). C) Mapping resting state networks as outlined by the Cole-Anticevic Brain Network Parcellation. (For interpretation of the references to color in this figure legend, the reader is referred to the web version of this article.)

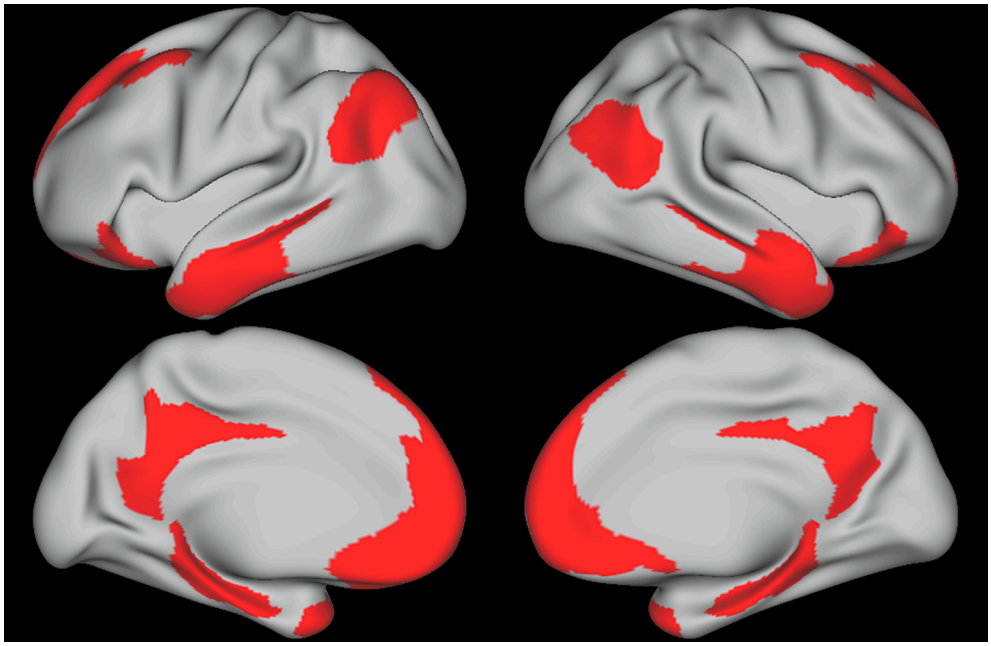

Fig. 4. The DMN network consists of the medial prefrontal cortex, posterior cingulate cortex, inferior parietal cortex and precuneus.

Table 2
Global efficiency of network in LBP. rsFC data was used to compile binary undirected networks for each resting state network that had been thresholded within a network density range of 15%-30% in steps of 2.5%. The corresponding global efficiency scores for each network rsFC matrix were averaged across thresholds. A Wilcoxon rank-sum test was used to assess the statistical significance and the corresponding z values recorded. (* = $p < 0.05$, uncorrected).

Network Names	Z-Value	p-Value
Primary Visual	1.60	0.110
Secondary Visual	1.30	0.180
Somatomotor	0.0850	0.930
Cingulo-Opercular	−0.580	0.560
Dorsal Attention	0.410	0.680
Language	0.330	0.750
Frontoparietal	−1.80	0.0690
Auditory	−0.590	0.550
Default Mode	*−2.10*	*0.0320**
Posterior-Multimodal	1.20	0.230
Ventral-Multimodal	1.90	0.0640
Orbito-Affective	−0.12	0.910

2006) and facial expression of pain (Simon et al., 2006). Based on our findings, we believe these regions may also be involved in the affective component of LBP (Vogt, 2005).

4.2. Visual network plasticity during LBP

In humans, spatial navigation is a complex process that involves the processing of multiple incoming sensory stimuli based on surrounding spatial landmarks to determine the optimal route to a specific goal (Brodbeck and Tanninen, 2012). In a recent systematic review (Tong et al., 2017), one factor common to all chronic LBP patients was impaired proprioception. Impaired proprioception was also far worse in patients with severe chronic LBP (Mitchell et al., 2009; Sheeran et al., 2012). Proprioception is an important sensory input that functions to provide perception of the body (i.e. physical self-awareness) and judgement of alignment relative to one's environment (Moseley, 2008). Due to impaired cortical processing of proprioceptive input, patients with chronic LBP exhibit aberrant perception, and consequently alignment of their bodies relative to their surroundings (Wand et al., 2011).

To compensate for proprioception impairment, vision becomes the next reliable sensory feedback that helps in spatial orientation, movement coordination, and balance (Guerraz et al., 2001). In patients with chronic LBP, several studies have demonstrated that dependence on visual input increases in order to maintain a vertical posture (Brumagne et al., 2000; Mann et al., 2010; Mazibrada et al., 2008). When visual input is removed or reduced, patients with chronic LBP have increased postural sway and loss of balance (Mann et al., 2010; Mok et al., 2004). These studies support the visual dependence in patients with chronic

Table 3
A summary of the classification accuracy and AUC when cortical thickness was used to train the SVM model.

SVM (LOO)	Accuracy	Sensitivity	Specificity	AUC
LBP vs HC	74.51%	74.07%	75.00%	0.787

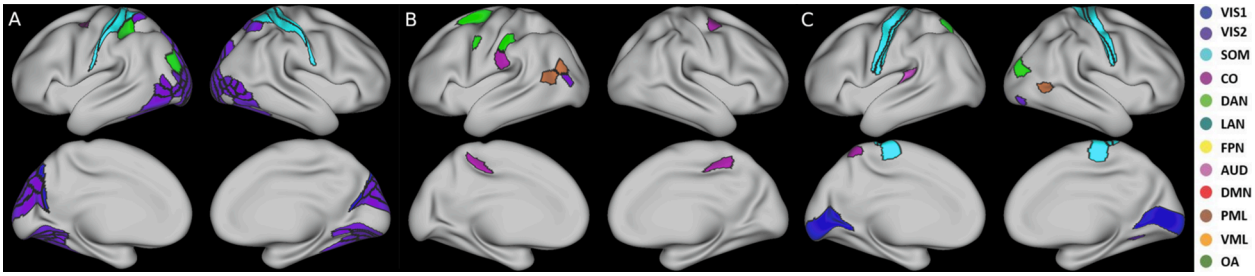

Fig. 5. Hubs that were A) common to LBP and HC, B) common to HC but not to LBP patients, and C) common to LBP patients but not to HC.

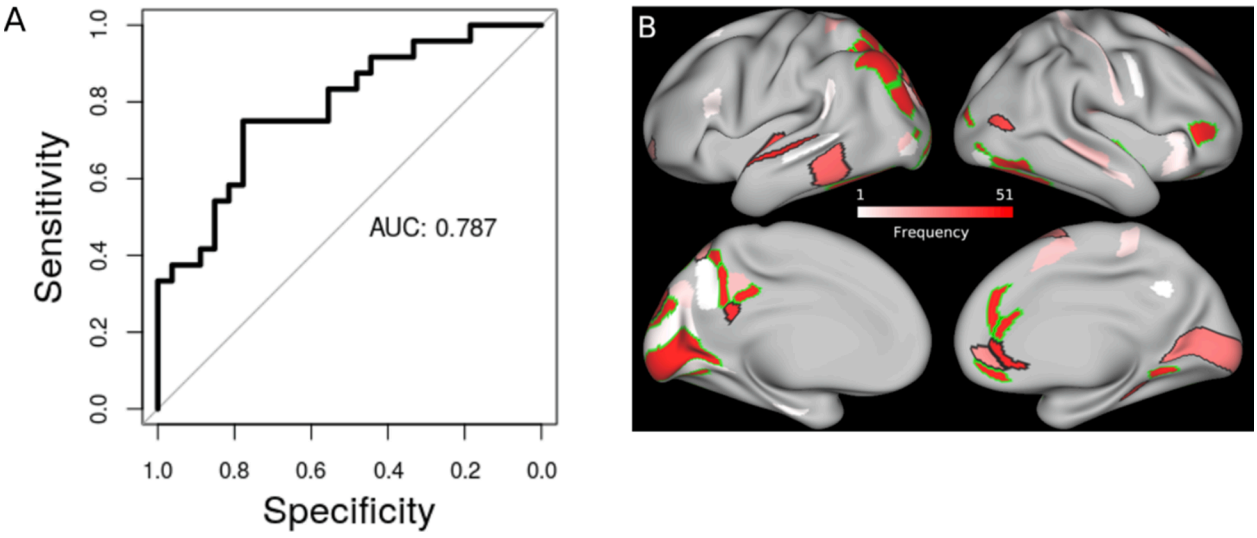

Fig. 6. Machine learning to predict LBP. A) Receiver Operating Characteristic (ROC) curve plot for the LBP vs HC classification. B) Frequency of parcels used to train the SVM model using cortical thickness. Parcels outlined in black are the top 40 most frequently contributing parcels to the classification of patient group when using CT. Parcels outlined in green have the highest frequency (51, i.e., selected as features in all LOO iterations) when contributing to the classification of all patients. (For interpretation of the references to color in this figure legend, the reader is referred to the web version of this article.)

LBP. Within our LBP cohort, we found multiple parcels from the visual networks were highly predictive of LBP when using a classification algorithm trained using CT (Fig. 6**B** and ***Supplementary Information, Table S12)***. We also found multiple increases in connectivity between the visual networks and other RSNs. These increases in connectivity could be a result of the visual system prioritizing tasks such as maintaining verticality and posture while placing less emphasis on the control of attentional tasks. The presence of the primary visual cortex as a hub in LBP patients and not in HC is essential in coordinating this increase in network processing and information exchange to aid in proprioception.

4.3. Role of the DMN network in LBP

Chronic pain is an attention demanding process, often competing with other external stimuli for cognitive resources (Eccleston and Crombez, 1999). In fact, individuals across many chronic pain states show deficits in attention (Grisart and Van der Linden, 2001; Van Damme et al., 2010). The default mode network (DMN) is composed of many higher order cognitive processing regions including the medial prefrontal cortex, posterior cingulate cortex, inferior parietal cortex and precuneus (Raichle et al., 2001; Shulman et al., 1997). While it is still unclear what the DMN is responsible for, elements of its networks have been implicated in episodic memory (Zysset et al., 2002), modulation of pain perception (Kucyi et al., 2013), and monitoring the external environment (Buckner et al., 2008; Raichle et al., 2001). There have been many recent studies which support the reorganization of DMN function across many chronic pain states (Baliki et al., 2014, 2008; Tagliazucchi et al., 2010).

In this study, several parcels from the DMN were highly predictive of LBP when using a classification algorithm trained using CT (Fig. 6**B** and ***Supplementary Information, Table S12)***. The DMN also showed increased (both significant and non-significant) connectivity with most other RSNs in LBP patients. However, the DMN showed a significant decrease in connectivity with nodes within its own network in LBP patients. In addition, there was a significant decrease in network efficiency of the DMN. Executive functions are laborsome requiring the availability of resources which is achieved by reducing the activation of the DMN (Hernández-Álvarez et al., 2020). A decrease in the efficiency of the DMN in LBP patients might affect the induced deactivation of this network and hence compromise their executive functions (Satterthwaite et al., 2013). Recent data from patients with Alzheimer's disease (Brown, 2017) and attention-deficit/hyperactivity disorder (Liddle et al., 2011) show the role of the DMN in executive function deficit. This decrease in network efficiency explains the hyperactive connectivity we observe between the DMN and all other RSNs in LBP patients.

4.4. Hub reorganization in sensorimotor processing

Of primary importance is the role of the bilateral primary motor cortex in regulating the flow of information specifically by acting as a hub within LBP patients but not HC. The motor cortex has been implicated in a number of functions beyond motor control such as visuomotor transformations (Georgopoulos and Pellizzer, 1995), language processing (Moseley et al., 2012), memory retrieval (Kaas et al., 2007), and pain processing (Vogt, 2005). It has been proposed that an incongruence between motor intention and movement, or sensorimotor conflict, is responsible for increased activation of M1 (Roussel et al., 2013). Systems responsible for motor function are closely linked to sensory feedback systems, which are monitored to detect deviations from the predicted response (Frith et al., 2000). In HC, presenting conflicting information, such as a mismatch between intention, proprioception, or visual feedback induced pain and sensory disturbances (Daenen et al., 2010; McCabe et al., 2005) and aggravated symptoms in those with chronic pain (Daenen et al., 2012).

Patients with chronic LBP frequently experience proprioception deficits (Brumagne et al., 2000) and tactile acuity deficits (Luomajoki and Moseley, 2011). A hyper-efficient posterior multimodal network combined with abnormal proprioceptive representation of the lower back in the primary somatosensory cortex (Wand et al., 2011) may contribute to sensorimotor conflicts in patients with chronic LBP. The lack of visual input of moving segments (Harris, 1999; Wand et al., 2011) and reduced activity in vision processing centers can enhance sensorimotor conflicts, as vision is the dominant form of perception (Jeannerod, 2003). In addition, the lack of visual feedback means that atypical cortical proprioceptive representation cannot be corrected (Wand et al., 2011). These alterations in proprioceptive representation, visual perception, and sensorimotor conflicts lead to downstream effects in higher order pain processing centers which may directly produce pain and sustain altered motor control strategies.

4.5. SVM classifier trained using cortical thickness

A clinically usable finding in this study is the development of a machine learning classification engine that can predict patient group based on differences in cortical thickness. Recent studies have attempted to predict patient group in chronic pain states using structural features (Bagarinao et al., 2014; Sevel et al., 2018; Ung et al., 2014). However, this is the first study to demonstrate the advantage of using structural features derived from brain imaging parcellated using an MMP when discerning between LBP and HC patient groups. We trained the classifier using CT which achieved a maximum classification accuracy of 74.51% (AUC = 0.787, 95% CI: 0.66–0.91). The results validated our hypothesis that widespread changes in CT can be used as an imaging biomarker for LBP to guide therapy.

5. Limitations

We did not explore subcortical areas as the HCP's MMP only includes cortical areas. Despite our attempts to recruit a homogenous population of subjects without a history of spine surgery, we were met with difficulty, as chronic LBP presents as a syndrome with numerous etiologies, wide variability, and countless affecting features. The pitfalls of the machine learning methods include, but are not limited to, incomplete, biased data or noisy datasets and overfitting. Solutions include recruiting larger matched samples and testing the models on unseen data. Due to a relatively small sample size and high number of parcels (360), many of our results were significant only at uncorrected levels and therefore should be considered with due caution. Finally, pain and emotion are inherently subjective metrics that depend on the patient population.

6. Conclusion

In conclusion, our results suggest that low back pain is associated with widespread structural and functional changes in the brain. Our data shows that localized structural changes are correlated with clinical pain and emotional measures. The resting state functional connectivity and graph theory network approaches also support the findings of alterations of brain structure and functions localized to regions corresponding to cognitive functions, visuo-motor and affective dimensions of pain processing. Importantly, our results also demonstrate how machine-assisted classification algorithms can accurately categorize patient specific data into their respective cohort using data derived from a multi-modal parcellation.

CRediT authorship contribution statement

Bidhan Lamichhane: Conceptualization, Data collection, Methodology, Investigation, Data analysis, Visualization, Writing - original draft, Validation, Writing - review & editing. **Dinal Jayasekera:** Conceptualization, Data collection, Methodology, Investigation, Data analysis, Visualization, Writing - original draft, Validation, Writing - review & editing. **Rachel Jakes:** Data analysis, Writing - original draft, Validation, Writing - review & editing. **Matthew F. Glasser:** Data analysis, Validation, Writing - review & editing. **Justin Zhang:** Data analysis, Validation, Writing - review & editing. **Chunhui Yang:** Data analysis, Validation, Writing - review & editing. **Derayvia Grimes:** Data curation, Project management, Validation, Writing - review & editing. **Tyler L. Frank:** Data curation, Project management, Validation, Writing - review & editing. **Wilson Z. Ray:** Supervision, Validation, Writing - review & editing. **Eric C. Leuthardt:** Supervision, Validation, Writing - review & editing. **Ammar H. Hawasli:** Conceptualization, Data curation, Funding acquisition, Supervision, Resources, Software, Validation, Writing - review & editing.

Declaration of Competing Interest

The authors declare that they have no known competing financial interests or personal relationships that could have appeared to influence the work reported in this paper.

Acknowledgments

The authors would like to thank Timothy Coalson for his support with troubleshooting outputs from the HCP's pre-processing pipeline and Connectome Workbench. They also appreciate the managing staff at the Mallinckrodt Institute of Radiology Washington University in St. Louis: Linda Hood and Glenn Foster, for help with MRI acquisition.

Funding

This work was supported by the Cervical Spine Research Society, Neurosurgery Research and Education Foundation and the Barnes-Jewish Hospital Foundation. The content of this article is solely the responsibility of the authors and does not necessarily represent the official views of the funding agencies.

Appendix A. Supplementary data

Supplementary data to this article can be found online at https://doi.org/10.1016/j.nicl.2020.102530.

References

Achard, S., Bullmore, E., 2007. Efficiency and cost of economical brain functional networks. PLoS Comput. Biol. 3, e17.
Achard, S., Delon-Martin, C., Vértes, P.E., Renard, F., Schenck, M., Schneider, F., Heinrich, C., Kremer, S., Bullmore, E.T., 2012. Hubs of brain functional networks are radically reorganized in comatose patients. Proc. Natl. Acad. Sci. 109, 20608–20613.
Apkarian, A.V., Sosa, Y., Sonty, S., Levy, R.M., Harden, R.N., Parrish, T.B., Gitelman, D. R., 2004. Chronic back pain is associated with decreased prefrontal and thalamic gray matter density. J. Neurosci. 24, 10410–10415.
Arbabshirani, M.R., Plis, S., Sui, J., Calhoun, V.D., 2017. Single subject prediction of brain disorders in neuroimaging: promises and pitfalls. Neuroimage 145, 137–165.
Arslan, A.K., Colak, C., Sarihan, M.E., 2016. Different medical data mining approaches based prediction of ischemic stroke. Comput. Methods Programs Biomed. 130, 87–92.
Bagarinao, E., Johnson, K.A., Martucci, K.T., Ichesco, E., Farmer, M.A., Labus, J., Ness, T. J., Harris, R., Deutsch, G., Apkarian, A.V., Mayer, E.A., Clauw, D.J., Mackey, S., 2014. Preliminary structural MRI based brain classification of chronic pelvic pain: a MAPP network study. Pain 155, 2502–2509. https://doi.org/10.1016/j.pain.2014.09.002.
Balenzuela, P., Chernomoretz, A., Fraiman, D., Cifre, I., Sitges, C., Montoya, P., Chialvo, D.R., 2010. Modular organization of brain resting state networks in chronic back pain patients. Front. Neuroinform. 4, 116.
Baliki, M.N., Geha, P.Y., Apkarian, A.V., Chialvo, D.R., 2008. Beyond feeling: chronic pain hurts the brain, disrupting the default-mode network dynamics. J. Neurosci. 28, 1398–1403.
Baliki, M.N., Mansour, A.R., Baria, A.T., Apkarian, A.V., 2014. Functional reorganization of the default mode network across chronic pain conditions. PLoS ONE 9, e106133.
Baliki, M.N., Petre, B., Torbey, S., Herrmann, K.M., Huang, L., Schnitzer, T.J., Fields, H. L., Apkarian, A.V., 2012. Corticostriatal functional connectivity predicts transition to chronic back pain. Nat. Neurosci. 15, 1117–1119.
Baliki, M.N., Schnitzer, T.J., Bauer, W.R., Apkarian, A.V., 2011. Brain morphological signatures for chronic pain. PLoS ONE 6.
Bassett, D.S., Nelson, B.G., Mueller, B.A., Camchong, J., Lim, K.O., 2012. Altered resting state complexity in schizophrenia. Neuroimage 59, 2196–2207.
Bernabéu-Sanz, Á., Mollá-Torró, J.V., López-Celada, S., Moreno López, P., Fernández-Jover, E., 2020. MRI evidence of brain atrophy, white matter damage, and functional adaptive changes in patients with cervical spondylosis and prolonged spinal cord compression. Eur. Radiol. 30, 357–369. https://doi.org/10.1007/s00330-019-06352-z.
Blum, A.L., Langley, P., 1997. Selection of relevant features and examples in machine learning. Artif. Intell. 97, 245–271. https://doi.org/10.1016/s0004-3702(97)00063-5.
Brodbeck, D.R., Tanninen, S.E., 2012. Place learning and spatial navigation. Encycl. Sci. Learn. Springer Sci. Bus. Media New York, NY, USA 2639–2641.
Brown, C.A., 2017. The default mode network and executive function: Influence of age, white matter connectivity, and Alzheimer's pathology.
Brumagne, S., Cordo, P., Lysens, R., Verschueren, S., Swinnen, S., 2000. The role of paraspinal muscle spindles in lumbosacral position sense in individuals with and without low back pain. Spine (Phila. Pa. 1976). 25, 989–994.
Buckner, R.L., Andrews-Hanna, J.R., Schacter, D.L., 2008. The brain's default network: anatomy, function, and relevance to disease.
Burgmer, M., Gaubitz, M., Konrad, C., Wrenger, M., Hilgart, S., Heuft, G., Pfleiderer, B., 2009. Decreased gray matter volumes in the cingulo-frontal cortex and the amygdala in patients with fibromyalgia. Psychosom. Med. 71, 566–573.
Carrera, E., Tononi, G., 2014. Diaschisis: past, present, future. Brain 137, 2408–2422. https://doi.org/10.1093/brain/awu101.
Crossley, N.A., Mechelli, A., Scott, J., Carletti, F., Fox, P.T., McGuire, P., Bullmore, E.T., 2014. The hubs of the human connectome are generally implicated in the anatomy of brain disorders. Brain 137, 2382–2395.
Daenen, L., Nijs, J., Roussel, N., Wouters, K., Van Loo, M., Cras, P., 2012. Sensorimotor incongruence exacerbates symptoms in patients with chronic whiplash associated disorders: an experimental study. Rheumatology 51, 1492–1499.
Daenen, L., Roussel, N., Cras, P., Nijs, J., 2010. Sensorimotor incongruence triggers sensory disturbances in professional violinists: an experimental study. Rheumatology 49, 1281–1289.
De Pauw, R., Aerts, H., Siugzdaite, R., Meeus, M., Coppieters, I., Caeyenberghs, K., Cagnie, B., 2020. Hub disruption in patients with chronic neck pain: a graph analytical approach. Pain 161, 729–741.
Dieleman, J.L., Baral, R., Birger, M., Bui, A.L., Bulchis, A., Chapin, A., Hamavid, H., Horst, C., Johnson, E.K., Joseph, J., 2016. US spending on personal health care and public health, 1996–2013. JAMA 316, 2627–2646.
Eccleston, C., Crombez, G., 1999. Pain demands attention: a cognitive–affective model of the interruptive function of pain. Psychol. Bull. 125, 356.
Erk, S., Abler, B., Walter, H., 2006. Cognitive modulation of emotion anticipation. Eur. J. Neurosci. 24, 1227–1236.
Farivar, S.S., Cunningham, W.E., Hays, R.D., 2007. Correlated physical and mental health summary scores for the SF-36 and SF-12 Health Survey, V. 1. Health Qual. Life Outcomes 5, 54.
Fischl, B., Dale, A.M., 2000. Measuring the thickness of the human cerebral cortex from magnetic resonance images. Proc. Natl. Acad. Sci. 97, 11050–11055.
Fornito, A., Zalesky, A., Bullmore, E., 2016. Fundamentals of brain network analysis. Academic Press.
Frith, C.D., Blakemore, S.-J., Wolpert, D.M., 2000. Abnormalities in the awareness and control of action. Philos. Trans. R Soc. London. Ser. B Biol. Sci. 355, 1771–1788.
Georgopoulos, A.P., Pellizzer, G., 1995. The mental and the neural: psychological and neural studies of mental rotation and memory scanning. Neuropsychologia 33, 1531–1547.
Ginestet, C.E., Nichols, T.E., Bullmore, T., Simmons, A., 2011. Brain network analysis: separating cost from topology using cost-integration. PLoS One 6.
Glasser, M.F., Coalson, T.S., Bijsterbosch, J.D., Harrison, S.J., Harms, M.P., Anticevic, A., Van Essen, D.C., Smith, S.M., 2019. Classification of temporal ICA components for separating global noise from fMRI data: Reply to Power. Neuroimage 197, 435–438.
Glasser, M.F., Coalson, T.S., Bijsterbosch, J.D., Harrison, S.J., Harms, M.P., Anticevic, A., Van Essen, D.C., Smith, S.M., 2018. Using temporal ICA to selectively remove global noise while preserving global signal in functional MRI data. Neuroimage 181, 692–717.
Glasser, M.F., Coalson, T.S., Robinson, E.C., Hacker, C.D., Harwell, J., Yacoub, E., Ugurbil, K., Andersson, J., Beckmann, C.F., Jenkinson, M., 2016a. A multi-modal parcellation of human cerebral cortex. Nature 536, 171–178.
Glasser, M.F., Smith, S.M., Marcus, D.S., Andersson, J.L.R., Auerbach, E.J., Behrens, T.E. J., Coalson, T.S., Harms, M.P., Jenkinson, M., Moeller, S., 2016b. The human connectome project's neuroimaging approach. Nat. Neurosci. 19, 1175.
Glasser, M.F., Sotiropoulos, S.N., Wilson, J.A., Coalson, T.S., Fischl, B., Andersson, J.L., Xu, J., Jbabdi, S., Webster, M., Polimeni, J.R., 2013. The minimal preprocessing pipelines for the Human Connectome Project. Neuroimage 80, 105–124.
Grachev, I.D., Fredrickson, B.E., Apkarian, A.V., 2002. Brain chemistry reflects dual states of pain and anxiety in chronic low back pain. J. Neural Transm. 109, 1309–1334.

Greve, D.N., Fischl, B., 2018. False positive rates in surface-based anatomical analysis. Neuroimage 171, 6–14.
Grisart, J.M., Van der Linden, M., 2001. Conscious and automatic uses of memory in chronic pain patients. Pain 94, 305–313.
Guerraz, M., Yardley, L., Bertholon, P., Pollak, L., Rudge, P., Gresty, M.A., Bronstein, A. M., 2001. Visual vertigo: symptom assessment, spatial orientation and postural control. Brain 124, 1646–1656.
Guyon, I., Weston, J., Barnhill, S., Vapnik, V., 2002. Gene selection for cancer classification using support vector machines. Mach. Learn. 46, 389–422.
Hall, M.A., Smith, L.A., 1998. Practical feature subset selection for machine learning.
Harris, A.J., 1999. Cortical origin of pathological pain. Lancet 354, 1464–1466.
Hashmi, J.A., Baliki, M.N., Huang, L., Baria, A.T., Torbey, S., Hermann, K.M., Schnitzer, T.J., Apkarian, A.V., 2013. Shape shifting pain: chronification of back pain shifts brain representation from nociceptive to emotional circuits. Brain 136, 2751–2768.
Hernández-Álvarez, D.M., Pacheco, L., Velasco-Segura, R., Perez De La Mora, M., Tejeda-Romero, C., González-García, N., 2020. Default mode network efficiency is correlated with deficits in inhibition in adolescents with inhalant use disorder. Front. Psychiatry 11, 209.
Jeannerod, M., 2003. The mechanism of self-recognition in humans. Behav. Brain Res. 142, 1–15.
Ji, J.L., Spronk, M., Kulkarni, K., Repovš, G., Anticevic, A., Cole, M.W., 2019. Mapping the human brain's cortical-subcortical functional network organization. Neuroimage 185, 35–57.
Kaas, A.L., Van Mier, H., Goebel, R., 2007. The neural correlates of human working memory for haptically explored object orientations. Cereb. Cortex 17, 1637–1649.
Kaplan, C.M., Schrepf, A., Vatansever, D., Larkin, T.E., Mawla, I., Ichesco, E., Kochlefl, L., Harte, S.E., Clauw, D.J., Mashour, G.A., 2019. Functional and neurochemical disruptions of brain hub topology in chronic pain. Pain 160, 973.
Kim, J.H., Suh, S.-I., Seol, H.Y., Oh, K., Seo, W.K., Yu, S.W., Park, K.W., Koh, S.B., 2008. Regional grey matter changes in patients with migraine: a voxel-based morphometry study. Cephalalgia 28, 598–604.
Kohavi, R., John, G.H., 1997. Wrappers for feature subset selection. Artif. Intell. 97, 273–324.
Kong, J., Spaeth, B., Wey, H.-Y., Cheetham, A., Cook, A.H., Jensen, K., Tan, Y., Liu, H., Wang, D., Loggia, M.L., 2013. S1 is associated with chronic low back pain: a functional and structural MRI study. Mol. Pain 9, 1744–8069.
Kucyi, A., Salomons, T.V., Davis, K.D., 2013. Mind wandering away from pain dynamically engages antinociceptive and default mode brain networks. Proc. Natl. Acad. Sci. 110, 18692–18697.
Kuhn, M., 2008. Building Predictive Models in R Using the caret Package. J. Stat. Software; Vol 1, Issue 5 . https://doi.org/10.18637/jss.v028.i05.
Last, A.R., Hulbert, K., 2009. Chronic low back pain: evaluation and management. Am. Fam. Physician 79, 1067–1074.
Latora, V., Marchiori, M., 2001. Efficient behavior of small-world networks. Phys. Rev. Lett. 87, 198701.
Letzen, J.E., Robinson, M.E., 2017. Negative mood influences default mode network functional connectivity in chronic low back pain patients: implications for functional neuroimaging biomarkers. Pain 158, 48.
Liddle, E.B., Hollis, C., Batty, M.J., Groom, M.J., Totman, J.J., Liotti, M., Scerif, G., Liddle, P.F., 2011. Task-related default mode network modulation and inhibitory control in ADHD: effects of motivation and methylphenidate. J. Child Psychol. Psychiatry 52, 761–771.
Liu, J., Zhao, L., Li, G., Xiong, S., Nan, J., Li, J., Yuan, K., von Deneen, K.M., Liang, F., Qin, W., 2012. Hierarchical alteration of brain structural and functional networks in female migraine sufferers. PLoS ONE 7.
Luomajoki, H., Moseley, G.L., 2011. Tactile acuity and lumbopelvic motor control in patients with back pain and healthy controls. Br. J. Sports Med. 45, 437–440.
Lutz, J., Jäger, L., de Quervain, D., Krauseneck, T., Padberg, F., Wichnalek, M., Beyer, A., Stahl, R., Zirngibl, B., Morhard, D., 2008. White and gray matter abnormalities in the brain of patients with fibromyalgia: a diffusion-tensor and volumetric imaging study. Arthritis Rheum. Off. J. Am. Coll. Rheumatol. 58, 3960–3969.
Lynall, M.-E., Bassett, D.S., Kerwin, R., McKenna, P.J., Kitzbichler, M., Muller, U., Bullmore, E., 2010. Functional connectivity and brain networks in schizophrenia. J. Neurosci. 30, 9477–9487.
Mann, L., Kleinpaul, J.F., Moro, A.R.P., Mota, C.B., Carpes, F.P., 2010. Effect of low back pain on postural stability in younger women: influence of visual deprivation. J. Bodyw. Mov. Ther. 14, 361–366.
Mansour, A., Baria, A.T., Tetreault, P., Vachon-Presseau, E., Chang, P.-C., Huang, L., Apkarian, A.V., Baliki, M.N., 2016. Global disruption of degree rank order: a hallmark of chronic pain. Sci. Rep. 6, 34853.
Martucci, K.T., Mackey, S.C., 2018. Neuroimaging of PainHuman evidence and clinical relevance of central nervous system processes and modulation. Anesthesiol. J. Am. Soc. Anesthesiol. 128, 1241–1254.
Mazibrada, G., Tariq, S., Pérennou, D., Gresty, M., Greenwood, R., Bronstein, A.M., 2008. The peripheral nervous system and the perception of verticality. Gait Posture 27, 202–208.
McCabe, C.S., Haigh, R.C., Halligan, P.W., Blake, D.R., 2005. Simulating sensory–motor incongruence in healthy volunteers: implications for a cortical model of pain. Rheumatology 44, 509–516.
Mitchell, T., O'Sullivan, P.B., Smith, A., Burnett, A.F., Straker, L., Thornton, J., Rudd, C. J., 2009. Biopsychosocial factors are associated with low back pain in female nursing students: a cross-sectional study. Int. J. Nurs. Stud. 46, 678–688.
Mok, N.W., Brauer, S.G., Hodges, P.W., 2004. Hip strategy for balance control in quiet standing is reduced in people with low back pain. Spine (Phila. Pa. 1976). 29, E107–E112.
Moseley, G.L., 2008. I can't find it! Distorted body image and tactile dysfunction in patients with chronic back pain. Pain 140, 239–243.
Moseley, R., Carota, F., Hauk, O., Mohr, B., Pulvermüller, F., 2012. A role for the motor system in binding abstract emotional meaning. Cereb. Cortex 22, 1634–1647.
Qiao, C., Lu, L., Yang, L., Kennedy, P.J., 2019. Identifying brain abnormalities with schizophrenia based on a hybrid feature selection technology. Appl. Sci. 9, 2148.
Raichle, M.E., MacLeod, A.M., Snyder, A.Z., Powers, W.J., Gusnard, D.A., Shulman, G.L., 2001. A default mode of brain function. Proc. Natl. Acad. Sci. 98, 676–682.
Robinson, E.C., Garcia, K., Glasser, M.F., Chen, Z., Coalson, T.S., Makropoulos, A., Bozek, J., Wright, R., Schuh, A., Webster, M., 2018. Multimodal surface matching with higher-order smoothness constraints. Neuroimage 167, 453–465.
Rocca, M.A., Ceccarelli, A., Falini, A., Colombo, B., Tortorella, P., Bernasconi, L., Comi, G., Scotti, G., Filippi, M., 2006. Brain gray matter changes in migraine patients with T2-visible lesions: a 3-T MRI study. Stroke 37, 1765–1770.
Roussel, N.A., Nijs, J., Meeus, M., Mylius, V., Fayt, C., Oostendorp, R., 2013. Central sensitization and altered central pain processing in chronic low back pain: fact or myth? Clin. J. Pain 29, 625–638.
Rubinov, M., Sporns, O., 2010. Complex network measures of brain connectivity: uses and interpretations. Neuroimage 52, 1059–1069.
Rubinstein, S.M., van Tulder, M., 2008. A best-evidence review of diagnostic procedures for neck and low-back pain. Best Pract. Res. Clin. Rheumatol. 22, 471–482.
Rudisch, A., Kremser, C., Peer, S., Kathrein, A., Judmaier, W., Daniaux, H., 1998. Metallic artifacts in magnetic resonance imaging of patients with spinal fusion: a comparison of implant materials and imaging sequences. Spine (Phila. Pa. 1976). 23, 692–699.
Ruscheweyh, R., Deppe, M., Lohmann, H., Stehling, C., Flöel, A., Ringelstein, E.B., Knecht, S., 2011. Pain is associated with regional grey matter reduction in the general population. PAIN® 152, 904–911.
Saeys, Y., Inza, I., Larrañaga, P., 2007. A review of feature selection techniques in bioinformatics. Bioinformatics 23, 2507–2517.
Satterthwaite, T.D., Wolf, D.H., Erus, G., Ruparel, K., Elliott, M.A., Gennatas, E.D., Hopson, R., Jackson, C., Prabhakaran, K., Bilker, W.B., 2013. Functional maturation of the executive system during adolescence. J. Neurosci. 33, 16249–16261.
Schmidt-Wilcke, T., Leinisch, E., Straube, A., Kämpfe, N., Draganski, B., Diener, H.C., Bogdahn, U., May, A., 2005. Gray matter decrease in patients with chronic tension type headache. Neurology 65, 1483–1486.
Schwarz, A.J., McGonigle, J., 2011. Negative edges and soft thresholding in complex network analysis of resting state functional connectivity data. Neuroimage 55, 1132–1146. https://doi.org/10.1016/j.neuroimage.2010.12.047.
Sevel, L.S., Boissoneault, J., Letzen, J.E., Robinson, M.E., Staud, R., 2018. Structural brain changes versus self-report: machine-learning classification of chronic fatigue syndrome patients. Exp. Brain Res. 236, 2245–2253.
Sheeran, L., Sparkes, V., Caterson, B., Busse-Morris, M., van Deursen, R., 2012. Spinal position sense and trunk muscle activity during sitting and standing in nonspecific chronic low back pain: classification analysis. Spine (Phila. Pa. 1976). 37, E486–E495.
Shen, W., Tu, Y., Gollub, R.L., Ortiz, A., Napadow, V., Yu, S., Wilson, G., Park, J., Lang, C., Jung, M., 2019. Visual network alterations in brain functional connectivity in chronic low back pain: a resting state functional connectivity and machine learning study. NeuroImage Clin. 22, 101775.
Shulman, G.L., Corbetta, M., Buckner, R.L., Fiez, J.A., Miezin, F.M., Raichle, M.E., Petersen, S.E., 1997. Common blood flow changes across visual tasks: I. Increases in subcortical structures and cerebellum but not in nonvisual cortex. J. Cogn. Neurosci. 9, 624–647.
Simon, D., Craig, K.D., Miltner, W.H.R., Rainville, P., 2006. Brain responses to dynamic facial expressions of pain. Pain 126, 309–318.
Stam, C.J., 2014. Modern network science of neurological disorders. Nat. Rev. Neurosci. 15, 683–695.
Supekar, K., Menon, V., Rubin, D., Musen, M., Greicius, M.D., 2008. Network analysis of intrinsic functional brain connectivity in Alzheimer's disease. PLoS Comput. Biol. 4.
Tagliazucchi, E., Balenzuela, P., Fraiman, D., Chialvo, D.R., 2010. Brain resting state is disrupted in chronic back pain patients. Neurosci. Lett. 485, 26–31.
Teutsch, S., Herken, W., Bingel, U., Schoell, E., May, A., 2008. Changes in brain gray matter due to repetitive painful stimulation. Neuroimage 42, 845–849.
Thomsen, M., Schneider, U., Breusch, S.J., Hansmann, J., Freund, M., 2001. Artefacts and ferromagnetism dependent on different metal alloys in magnetic resonance imaging. An experimental study. Orthopade 30, 540–544.
Tisdall, M.D., Hess, A.T., Reuter, M., Meintjes, E.M., Fischl, B., van der Kouwe, A.J.W., 2012. Volumetric navigators for prospective motion correction and selective reacquisition in neuroanatomical MRI. Magn. Reson. Med. 68, 389–399.
Tong, M.H., Mousavi, S.J., Kiers, H., Ferreira, P., Refshauge, K., van Dieën, J., 2017. Is there a relationship between lumbar proprioception and low back pain? A systematic review with meta-analysis. Arch. Phys. Med. Rehabil. 98, 120–136.
Ung, H., Brown, J.E., Johnson, K.A., Younger, J., Hush, J., Mackey, S., 2014. Multivariate classification of structural MRI data detects chronic low back pain. Cereb. Cortex 24, 1037–1044.
Vaccaro, A.R., Chesnut, R.M., Scuderi, G., Healy, J.F., Massie, J.B., Garfin, S.R., 1994. Metallic spinal artifacts in magnetic resonance imaging. Spine (Phila. Pa. 1976). 19, 1237–1242.
Valet, M., Gündel, H., Sprenger, T., Sorg, C., Mühlau, M., Zimmer, C., Henningsen, P., Tölle, T.R., 2009. Patients with pain disorder show gray-matter loss in pain-processing structures: a voxel-based morphometric study. Psychosom. Med. 71, 49–56.
Van Damme, S., Legrain, V., Vogt, J., Crombez, G., 2010. Keeping pain in mind: a motivational account of attention to pain. Neurosci. Biobehav. Rev. 34, 204–213.

van den Heuvel, M.P., Sporns, O., 2013. Network hubs in the human brain. Trends Cogn. Sci. 17, 683–696.
Vogt, B.A., 2005. Pain and emotion interactions in subregions of the cingulate gyrus. Nat. Rev. Neurosci. 6, 533–544.
Vos, T., Abajobir, A.A., Abate, K.H., Abbafati, C., Abbas, K.M., Abd-Allah, F., Abdulkader, R.S., Abdulle, A.M., Abebo, T.A., Abera, S.F., 2017. Global, regional, and national incidence, prevalence, and years lived with disability for 328 diseases and injuries for 195 countries, 1990–2016: a systematic analysis for the Global Burden of Disease Study 2016. Lancet 390, 1211–1259.
Wand, B.M., Parkitny, L., O'Connell, N.E., Luomajoki, H., McAuley, J.H., Thacker, M., Moseley, G.L., 2011. Cortical changes in chronic low back pain: current state of the art and implications for clinical practice. Man. Ther. 16, 15–20.
Ware, J.E., 1993. Scoring the SF-36. SF-36. Heal. Surv. Man. Interpret. Guid.
Ware, J.E., Kosinski, M., Keller, S.D., Kosinski, M.K., Keller, S.K., Ware, J, Keller, S., Ware, JEKM, Kosinki, M., Ware, J.E.J., 1994. SF-36 physical and mental health summary scales: a user's manual.
Ware Jr, J.E., Kosinski, M., Bayliss, M.S., McHorney, C.A., Rogers, W.H., Raczek, A., 1995. Comparison of methods for the scoring and statistical analysis of SF-36 health profile and summary measures: summary of results from the Medical Outcomes Study. Med. Care AS264–AS279.
Ware Jr, J.E., Sherbourne, C.D., 1992. The MOS 36-item short-form health survey (SF-36): I. Conceptual framework and item selection. Med. Care 473–483.
Wiech, K., Jbabdi, S., Lin, C.S., Andersson, J., Tracey, I., 2014. Differential structural and resting state connectivity between insular subdivisions and other pain-related brain regions. PAIN® 155, 2047–2055.
Yarkoni, T., Poldrack, R.A., Nichols, T.E., Van Essen, D.C., Wager, T.D., 2011. Large-scale automated synthesis of human functional neuroimaging data. Nat. Methods 8, 665.
Zysset, S., Huber, O., Ferstl, E., von Cramon, D.Y., 2002. The anterior frontomedian cortex and evaluative judgment: an fMRI study. Neuroimage 15, 983–991.